Slow Dielectric Relaxation of *cis*-Polyisoprene in a Polybutadiene Matrix. 1. Experimental Results on the Matrix Effect

Hiroshi Watanabe,* Manabu Yamazaki, Hirotsugu Yoshida, Keiichiro Adachi, and Tadao Kotaka

Department of Macromolecular Science, Faculty of Science, Osaka University, Toyonaka, Osaka 560, Japan

Received February 8, 1991; Revised Manuscript Received May 17, 1991

ABSTRACT: Dielectric normal mode relaxation was examined on *homogeneous* blends of a small amount of *cis*-polyisoprene (PI) and a large excess of polybutadiene (PB), both having a narrow molecular weight distribution (MWD). Two types of PI were used: One has dipoles along the chain contour all parallel in the same direction, and the other, dipoles with the direction inverted once at the center of the chain contour. The dielectric relaxation time τ_n of the probe PI entangled with the matrix PB decreased with decreasing matrix molecular weight M_{PB}. However, the relaxation mode distribution as revealed from the shape of the dielectric loss curves remained the same and universal for all systems examined. For the two types of PI chains of nearly the same length but with and without dipole inversion, the ratio of their τ_n's was insensitive to M_{PB}, in spite of significant decreases of their respective τ_n with decreasing M_{PB}. The relaxation behavior of the dilute probe PI chain in the blends was also compared with that of *narrow MWD* bulk PI. It turned out that the dielectric mode distributions and end-to-end distances of the PI chains were almost the same in the blends and in bulk. This result supports the previous suggestion of Adachi and Kotaka that the slow dielectric response of *bulk* PI systems reflects the motion of *individual* PI chains involved in the systems.

I. Introduction

Entanglements have a profound effect on the dynamics of condensed systems of long polymer chains.[1,2] Among the several molecular models proposed so far to describe their behavior,[3] the tube model of Doi and Edwards[4,5] appears to be most successful. However, there still exist nonnegligible disagreements between the model prediction and experiments on, for example, the viscosity (η)–molecular weight (M) relationship.[3,5,6] Within the framework of the generalized tube model, those disagreements were attributed to some additional relaxation mechanisms other than reptation: the contour length fluctuation[6,7] and constraint release[6,8,9] mechanisms that were not accounted in the original Doi–Edwards theory.

For binary blends composed of long and short linear polymer chains (with molecular weights M_L and M_S, respectively, and with narrow molecular weight distribution), the importance of the constraint release mechanism has been experimentally established for certain *extreme* cases: For long chains that were *dilute* in the blend and entangled only with *much shorter* matrix chains, the diffusion and viscoelastic relaxation times were found to be proportional to $M_L^2M_S^3$,[10–16] and the slow viscoelastic relaxation mode distribution, close to that for the Rouse dynamics.[10–14] These results were well described by the model for a *pure* constraint release mechanism proposed by Graessley,[6] who considered random local motion of the long chain induced by diffusion of the surrounding matrix chains.

However, as M_S approaches M_L, the diffusion and viscoelastic relaxation times were found to become more weakly dependent on M_S, and the relaxation mode distribution became narrower.[11,13–16] Those results suggest a competition of constraint release and reptation to be taking place, the former no longer overwhelming the latter as $M_S \to M_L$. For such competition, two types of models were already proposed.[6,17] However, we still need more critical experiments on blends with M_S approaching M_L so that we can better understand the binary blend dynamics.[17]

For this purpose, it is useful to examine the dielectric behavior of a particular type of polymer chains, classified as *type-A* chains by Stockmayer,[18] having components of dipoles aligned in the same direction along the chain contour. The global motion of such chains induces changes in polarization of the system and is dielectrically active. Dielectric measurements on type-A chains enable us to obtain information on an end-to-end vector correlation function, as was first demonstrated by Stockmayer and co-workers[18–20] and extensively examined by Adachi, Kotaka, and co-workers[21–30] and also by Boese, Kremer, and co-workers.[31,32] This function represents correlation of chain orientation *at two separate times* and is different in nature either from the orientation function representing anisotropy of chain orientation *at a given time* or from the segment displacement function related to *segment locations* at two separate times. If two or more relaxation mechanisms are competing with one another, the outcome of the competition is not necessarily the same for the three different microscopic functions mentioned above.[17] Thus as complementary to viscoelastic and diffusion measurements that provide information on the orientation and segment displacement functions, dielectric measurements on type-A chains are important to examine the binary blend dynamics, in particular for those with M_S approaching M_L.

From the viewpoint explained above, we have examined slow dielectric relaxation modes of type-A probe chains in blends. In the blends examined, the content of the probe chains was small so that they were entangled only with the matrix chains. Such blends are referred to as *dilute* blends. As the probe chains, we used linear *cis*-polyisoprene (PI), which were found to be type A by Adachi and Kotaka.[21,22] Specifically, two types of linear PI chains were used: One was those having dipoles along the chain contour in one direction and the other was that with inversion of the dipole direction at the center of the contour[30] as depicted in Figure 1. As the matrix, we used linear polybutadiene (PB), which has no dipole along the chain contour and is dielectrically inert (with a very small dielectric loss $\epsilon'' < 10^{-4}$) at long times. Because of this feature, PB chains are very convenient as the matrix for

0024-9297/91/2224-5365$02.50/0

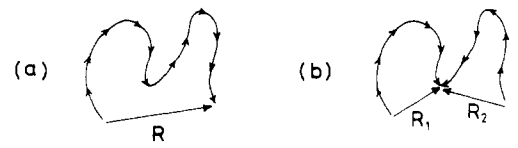

Figure 1. Schematic representation of linear *cis*-polyisoprenes (a) without and (b) with dipole inversion.

Table I
Characteristics of Polymer Samples

code	$10^{-3}M_w$	M_w/M_n
	Polyisoprenes[a]	
I-10	10.4	1.04
I-13	13.4	1.06
I-24	23.8	1.05
I-27[b]	27.3	1.06
I-35	35.4	1.06
2(I-13)[c]	26.2	1.06
	Polybutadienes[d]	
B-9	9.24	1.07
B-20	19.9	1.06
B-152	152	1.06

[a] Cis:trans:vinyl ≅ 75:20:5. [b] Used only for turbidity tests. [c] Sample 2(I-13) has dipole inversion;[30] the other PI samples are regular PI chains without dipole inversion. [d] Cis:trans:vinyl ≅ 40:50:10.

observing the dielectric response of a small amount of probe PI chains in the dilute blends.

In this paper, we present experimental results on dilute PI/PB blends and examine the effect of the motion of the matrix chains on the dynamics of the probe PI chains. These results are compared with previous results on bulk PI chains reported by Adachi, Kotaka, and co-workers.[21-30] In Part 2, the results obtained here will be quantitatively compared with the two models referred to as the configuration-independent and the configuration-dependent constraint release models.[6,17]

II. Experimental Section

Materials. Linear *cis*-polyisoprene (PI) samples were prepared by living anionic polymerization. First, a small fraction of a prescribed amount of isoprene (I) monomer was initiated with *sec*-butyllithium (*s*-BuLi) in heptane at 60 °C for 20 min (seeding reaction), and the remaining I monomer was then introduced into the reaction vessel and allowed to polymerize at room temperature for 48 h. After completion of the reaction, regular PI chains without dipole inversion (cf. Figure 1a) were recovered by terminating the living ends with methanol. Linear PI chains with dipole inversion (cf. Figure 1b) were prepared through the coupling of living PI precursor ends with a bifunctional terminator, *p*-xylylene dichloride ($ClCH_2C_6H_4CH_2Cl$), followed by successive fractionation. The details were described elsewhere.[30] Linear polybutadiene (PB) samples were prepared by anionic polymerization with *s*-BuLi in benzene at room temperature.

The weight-average molecular weight M_w and the heterogeneity index M_w/M_n were determined on a gel permeation chromatograph (Tosoh Co., Model HLC-801A) equipped with a combined refractometer plus light scattering photometer (Tosoh Co., Model LS-8000). Chloroform was the elution solvent. Whenever necessary, previously prepared and characterized PI samples[26,27] were used as elution standards. ^1H and ^{13}C NMR measurements revealed that the microstructure was cis:trans:vinyl ≅ 75:20:5 for the PI chains used and 40:50:10 for the PB chains.

Table I summarizes the characteristics of the samples used in this study. All samples have narrow molecular weight distributions ($M_w/M_n < 1.1$). The code number represents the M_w for the PB and regular PI chains and $M_w/2$ for the dipole-inverted PI chain, both in units of thousands. Samples I-24, I-27, and 2(I-13) have nearly the same length, and the former two do not but the last one does have the dipole inversion at the center of the chain contour.

Measurements. For blends of the PI (except I-27) and PB samples listed in Table I, dielectric measurements were carried out with a transformer bridge (General Radio, GR-1615A) at temperatures between 20 and 70 °C and frequencies from 50 Hz to 20 kHz in a helium atmosphere. The details of the measurements were described elsewhere.[26] To all the samples examined was added ~0.2 wt % of an antioxidant, butylhydroxytoluene (BHT), to prevent thermal degradation at high temperatures. The antioxidant did not disturb the dielectric measurements. For these systems the time–temperature superposition was applicable at the temperatures examined, and all data were reduced to 40 °C.

The PI/PB blends subjected to dielectric measurements contained ϕ_{PI} = 3 or 6 vol % of the PI samples. These blends were prepared in the following way. In each case, prescribed amounts of PI and PB samples were dissolved in cyclohexane to make a 5 wt % solution, which was freeze-dried at room temperature for 24 h and further dried at 35 °C under high vacuum for 24 h or more to thoroughly remove the solvent and obtain a transparent and homogeneous blend.

To ensure the homogeneity of the blends under the conditions of the dielectric experiments, phase separation behavior was examined in a temperature range of $20 \le T$ (°C) ≤ 82 for various PI/PB blends prepared by the above method. Among the I-24, 2(I-13), and I-27/PB blends having nearly the same M_{PI}, the behavior was examined most extensively for the I-27/PB blend as a representative system. Each PI/PB mixture was annealed under high vacuum at its respective T for 24 h. Then turbidity was examined by visual observation. This turbidity test was made first with decreasing T and then repeated several times with increasing and decreasing T, and no hysteresis was observed. The difference between the refractive indices of PI and PB is large enough to cause visible turbidity on phase separation, as reported by Hasegawa and co-workers.[33]

III. Global Molecular Motion and Dielectric Response

In general, the complex dielectric constant $\epsilon^* = \epsilon' - i\epsilon''$ of an isotropic system is written as[34]

$$\epsilon^* - \epsilon_\infty = -\Delta\epsilon \int_0^\infty \frac{d\Phi(t)}{dt} e^{-i\omega t}\, dt \qquad (1)$$

where ω is the angular frequency; ϵ_∞, the unrelaxed dielectric constant; $\Delta\epsilon$, the relaxation intensity; and $i^2 = -1$. $\Phi(t)$ is the autocorrelation function and is related to the polarization $\mathbf{P}(t)$ of the system as[34]

$$\Phi(t) = \langle \mathbf{P}(t)\cdot\mathbf{P}(0)\rangle / \langle P(0)^2\rangle \qquad (2)$$

Here $\langle ... \rangle$ represents an ensemble average.

The polarization $\mathbf{P}(t)$ is given by the sum of all dipoles involved in the system. For the *slow* dielectric relaxation due to the global motion of PI chains with dipoles μ parallel to the chain contour, we can write[24]

$$\langle \mathbf{P}(t)\cdot\mathbf{P}(0)\rangle = \sum_p \sum_{i,j} \langle \mu_i^p(t)\cdot\mu_j^p(0)\rangle + \sum_{p\neq q} \sum_{i,j} \langle \mu_i^p(t)\cdot\mu_j^q(0)\rangle \qquad (3)$$

where $\mu_i^p(t)$ is the dipole moment of the ith bond of the pth PI chain at time t. The first and second terms represent the correlation of two segments belonging to the same and different PI chains, respectively.

The dielectric relaxation process due to the global motion of type-A chains is referred to as the *dielectric normal mode process*.[21] For such processes, Adachi and Kotaka[24] suggested that the second term in eq 3 vanishes even for bulk PI and the dielectric response simply reflects the motion of individual chains. Then the relaxation inten-

sities $\Delta\epsilon_n$ for those processes can be written as[18,23,24]

$$\Delta\epsilon_n = 4\pi\phi_{PI}\rho N_A\mu_c^2 F\langle R^2\rangle/3kTM_{PI} \quad (1')$$

where ρ is the density of the system; kT, the thermal energy; N_A, the Avogadro number; μ_c, the dipole moment per unit contour length; F, the ratio of internal to external field strengths; and $\langle R^2\rangle$, the mean-square end-to-end distance of the chain. For the dielectric normal mode processes, F was found to be a constant (close to unity).[23] Then the dimension of a PI chain is examined through a reduced intensity $\rho^{-1}\phi_{PI}^{-1}M_{PI}\Delta\epsilon_n \propto \langle R^2\rangle$.[23,24,26] This feature enables us to examine whether the chain is in an unperturbed state or not, as shown in Figure 11.

When no correlation exists between the PI chains in a sense that the dot product $\mu_i^p(t)\cdot\mu_j^q(0)$ with $p \neq q$ (eq 3) assumes positive and negative values with the same probability, the second term in eq 3 vanishes and the dielectric normal mode relaxation simply reflects the motion of individual chains. The validity of this simplification should be higher for our dilute PI/PB blends than for bulk PIs, because of much smaller correlation between the small amount of PI chains in the former. We experimentally tested the validity for the blends by examining whether the dielectric relaxation time and mode distribution remain the same as PI content ($\phi_{PI} \ll 1$) is decreased while the relaxation intensity is proportional to ϕ_{PI} (cf. Figure 5).

On the basis of the above simplification, we may write the autocorrelation function for *regular* PI chains without dipole inversion as

$$\Phi(t) = \langle \mathbf{R}(t)\cdot\mathbf{R}(0)\rangle/\langle R^2\rangle \quad (4)$$

where $\mathbf{R}(t)$ is the end-to-end vector of the PI chain at time t. On the other hand, for PI chains with dipole inversion, correlation between the two end-to-center (end-to-inversion-point) vectors, $\mathbf{R}_1(t)$ and $\mathbf{R}_2(t)$, contributes to $\Phi(t)$, and eq 2 becomes

$$\Phi(t) = \langle \Delta\mathbf{R}(t)\cdot\Delta\mathbf{R}(0)\rangle/\langle R^2\rangle \quad (5)$$

where $\Delta\mathbf{R}(t) = \mathbf{R}_1(t) - \mathbf{R}_2(t)$. Here, we used a relation, $\langle\Delta R^2\rangle = \langle R^2\rangle$, valid for a Gaussian chain (cf. Figure 11).

Comparing eqs 4 and 5, we see that the molecular motion itself is the same but the dielectric response is different for regular and dipole-inverted PI chains of the same length. The dielectric normal mode process is due to the end-to-end vector fluctuation for the former but to the end-to-center vector fluctuation for the latter, as first demonstrated by Stockmayer and Baur.[18,19] The dipole inversion is in some sense similar to optical labeling.

IV. Results and Discussion

Phase Behavior. Figure 2 shows results of the turbidity tests on PI/PB blends as indicated. The results for the I-24, 2(I-13), and I-27/PB blends are shown together in parts c and d, and those for the I-13 and I-10/B-152 blends, in part a. (In parts c and d, the I-27/PB blends should be a little less miscible than the I-24 and 2(I-13)/PB blends, as judged from the small difference in M_{PI}.) The filled circles indicate turbid and thus phase-separated blends, and the unfilled ones, transparent and clear blends that are homogeneous as judged from the visual observation. The dotted lines indicate the conditions of the dielectric measurements conducted for the blends.

As can be seen in Figure 2, the phase behavior is dependent rather strongly on M_{PI} and M_{PB}.[35,36] The smaller the M_{PI} and/or M_{PB}, the more miscible the PI and PB chains are.[37] In particular, no two-phase regime was

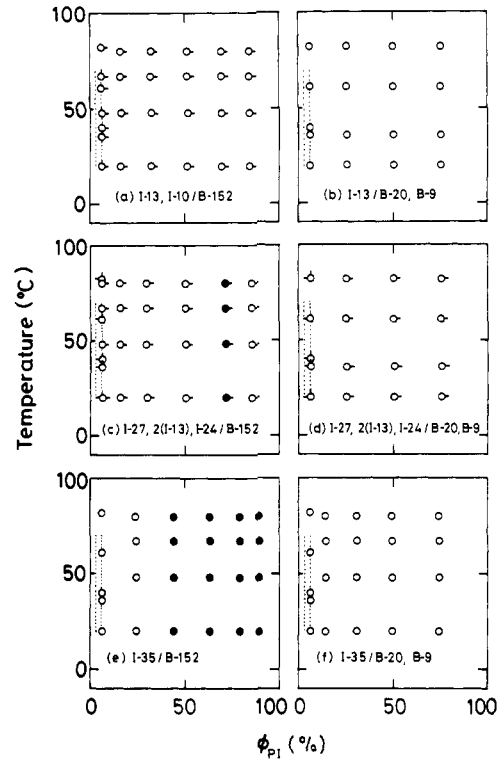

Figure 2. Results of turbidity tests for PI/PB blends as indicated. All blends contain ~0.2% of BHT (antioxidant). The unfilled circles indicate transparent and homogeneous blends, and the filled ones, turbid and phase-separated blends. The results for the I-13/B-152 and I-10/B-152 blends are shown in part a by circles with right pips and up pips, respectively; those for the I-27, 2(I-13), I-24/PB blends are shown in parts c and d by circles with right pips, up pips, and left pips, respectively. For the B-20 and B-9 blends with respective PI, the tests were made at common ϕ_{PI} and T, and the results are shown together in parts b, d, and f. The dotted lines indicate the conditions (ϕ_{PI} = 3 and 6 vol %, T = 20–70 °C) at which the dielectric measurements were conducted for the blends examined here (except for the I-27 blends that were used only for this turbidity test).

observed for the PI/B-20 and PI/B-9 blends at the T and ϕ_{PI} examined (parts b, d, and f). It should be noted that the dielectric measurements were made on the homogeneous blends at T and ϕ_{PI} (dotted lines) far from those for the two-phase regime. The PI chains in such blends would be in a (nearly) unperturbed state and have an (almost) Gaussian configuration, as suggested from results of small-angle neutron scattering measurements on some miscible blends.[38-42] In fact, those PI chains have (nearly) unperturbed dimensions, as shown in Figure 11.

Figure 3 shows the temperature dependence of the shift factor a_T (small unfilled circles) with which the time–temperature superposition of the ϵ'' curves was very well achieved for the PI/PB blends with small ϕ_{PI}. For comparison, Figure 3 also shows the shift factors for the viscoelastic quantities of dilute PI/PB blends and bulk PB (described in Part 2).

In Figure 3, we see that the a_T for ϵ'' of the PI/PB blends are entirely different from those for bulk PI[26] (the dashed curve) but are identical with those for bulk PB (the solid curve[43] and large unfilled circles). This result suggest that the segmental motion (or local friction) of the solute PI chains in the dilute blends is governed and activated by the PB segments. In other words, the PI segments are surrounded by PB segments, implying that PI chains are molecularly mixed with matrix PB chains.

The entanglement spacing M_e is 2×10^3 for bulk PB and 5×10^3 for bulk PI.[1] The M_e value for the probe PI

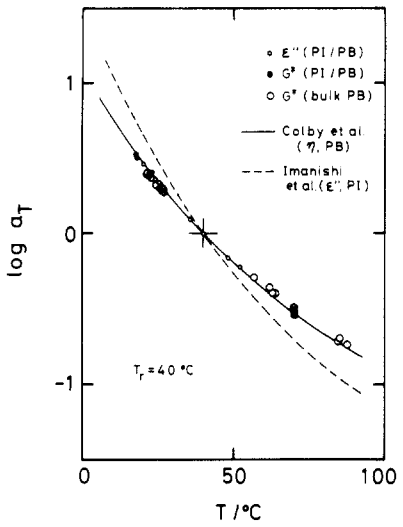

Figure 3. Temperature dependence of the shift factor a_T for the dielectric loss of dilute PI/PB blends (small unfilled circles). Small filled and large unfilled circles, respectively, represent a_T for the viscoelastic quantities of similar PI/PB blends and bulk PB systems. The solid curve represents a_T for the viscosity of bulk PBs reported by Colby and co-workers,[43] and the dashed curve, a_T for the dielectric loss of bulk PIs reported by Imanishi and co-workers.[26]

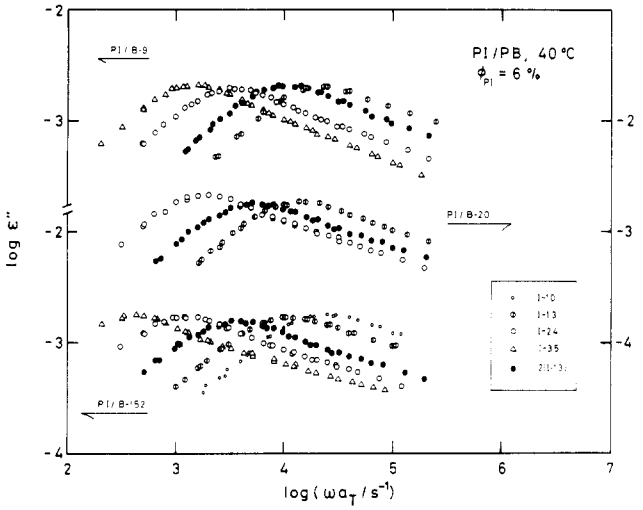

Figure 4. Master curves of dielectric loss ϵ'' reduced at 40 °C for PI/PB blends as indicated. The PI content is 6 vol % for all blends.

chains diluted in a PB matrix should be between these two values. Thus, the PI chains (with $10.4 \leq 10^{-3}M_{PI} \leq 35.4$ and $\phi_{PI} = 3$ and 6 vol %) in the dilute PI/PB blends are certainly entangled only with the matrix PB chains (with $10^{-3}M_{PB} \geq 9.24$).

Dielectric Loss Curves. Figure 4 compares the frequency dependence of ϵ'' reduced at 40 °C for various PI/PB blends with $\phi_{PI} = 6$ vol %. The matrix PB chains exhibit a very small dielectric loss ($\epsilon'' < 10^{-4}$) in this frequency range so that the ϵ'' of the blends is attributed to the dielectrically active PI chains. As seen in Figure 3, the segmental (local) motion of the probe PI chains in the blends is determined by the segmental motion of the matrix PB chains, which in turn is dependent only on temperature. Thus, the comparison of dynamic behavior of the probe PI chains at the reference temperature (=40 °C) is equivalent to the comparison at an isofriction state for the PI segments.

In Figure 4, we note that the relaxation of regular PI chains without dipole inversion (indicated by unfilled

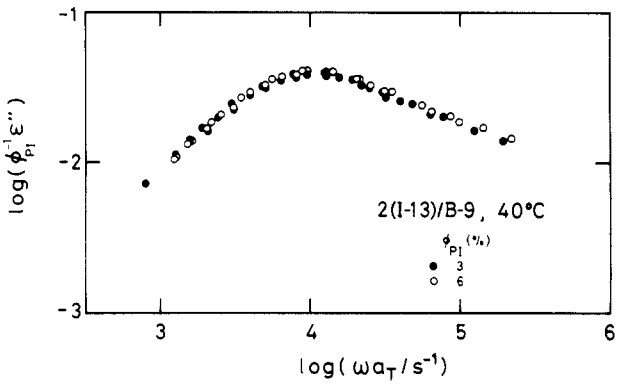

Figure 5. Comparison of the ϵ'' curves at 40 °C for 2(I-13)/B-9 blends with PI content $\phi_{PI} = 3$ (filled circles) and 6 vol % (unfilled circles). For comparison the ϵ'' curves are reduced by ϕ_{PI}.

symbols) becomes slower with increasing M_{PI}. Thus, the dielectric relaxation we are observing is due to the global motion of PI chains with an M_{PI}-dependent relaxation time.[44] We also note that the relaxation is considerably faster for the dipole-inverted 2(I-13) chain (filled circles) than for the regular I-24 chain (unfilled circles). The dipole inversion *filters* some of the normal modes that describe the global motion, as was demonstrated first by Baur and Stockmayer[18,19] and recently by ourselves.[30]

Figure 5 compares the ϵ'' curves reduced by ϕ_{PI} for 2(I-13)/B-9 blends with $\phi_{PI} = 3$ and 6 vol %. The curves coincide with each other. This concidence was found also for other dilute PI/PB blends examined in Figure 4. Those results indicate that the relaxation time and mode distribution are the same for the PI chains in the blends with different ϕ_{PI} (=3 and 6 vol %), and the relaxation intensity is proportional to ϕ_{PI}. In addition, these PI chains are in a (nearly) unperturbed state (cf. Figure 11). These results enable us to simplify eq 2 to eq 4 or 5 for the PI chains in the blends examined here, as anticipated. Thus, we can discuss the dielectric behavior of the PI/PB blends in terms of some relaxation mechanisms, as in the case of blends of chemically identical chains.

Relaxation Time. From the peak frequencies ω_{max} of the ϵ'' curves shown in Figure 4, we estimated the characteristic time τ_n for the dielectric normal mode process by

$$\tau_n = 1/\omega_{max} \tag{6}$$

As explained in a previous paper,[27] the relation between τ_n and the *longest* relaxation time τ_1 is dependent on the relaxation mode distribution. In principle, *only when* the systems being compared have the same mode distribution does a comparison of their τ_n give a meaningful result and correspond to the comparison of τ_1.[27] This is the case for the present blends as will be shown in Figures 8 and 9.

Figures 6 and 7, respectively, show the dependence of τ_n on M_{PB} of the matrix PB chains and on M_{PI} of the probe PI chains. The curves in the figures are arbitrarily drawn smooth curves through the data points and are only for helping examination of the data. In Figure 7, we multiplied τ_n for the dipole-inverted 2(I-13) chain by a factor of 4 and plotted against M_{PI} (=26.2×10^3) to compare with τ_n of the regular PI chains, as suggested in the previous work.[30]

In Figure 6, we see that the τ_n first increase with increasing M_{PB} and eventually level off. Correspondingly, as seen in Figure 7, the M_{PI} dependence of τ_n becomes stronger as M_{PI} (or M_{PI}/M_{PB} ratio) is decreased. These results clearly indicate that the relaxation of the probe chain is accelerated by the motion of sufficiently short matrix chains.[44] Within the framework of the generalized

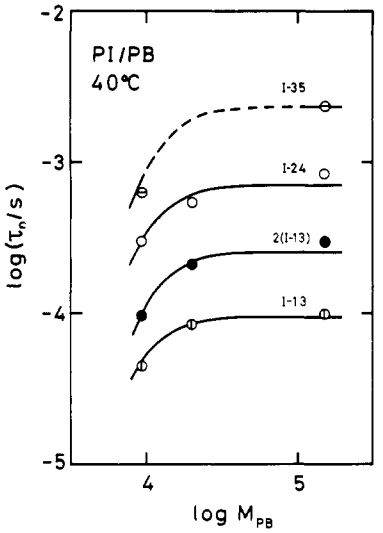

Figure 6. Dependence of dielectric relaxation time τ_n at 40 °C of probe PI chains on molecular weight M_{PB} of matrix PB chains.

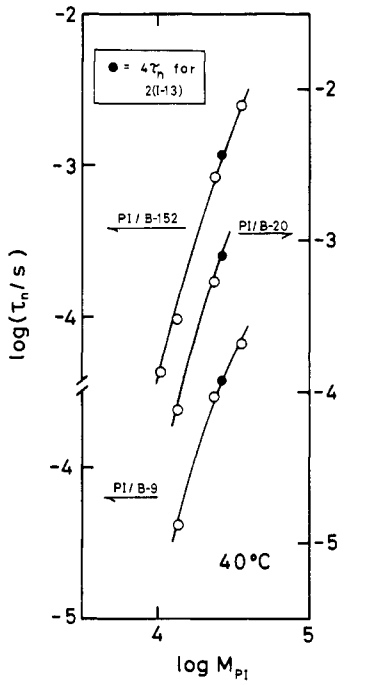

Figure 7. Dependence of dielectric relaxation time τ_n at 40 °C of probe PI chains on PI molecular weight M_{PI}. Filled circles represent τ_n multiplied by a factor of 4 for the dipole-inverted 2(I-13) chain.

tube model, this acceleration effect is attributable to the contribution of the constraint release mechanism to the dynamics of the probe chains.

In Figure 6, we also note that the ratio of τ_n's of the 2(I-13) and I-24 chains having nearly the same M_{PI} is insensitive to M_{PB}, in spite of the significant decrease of the respective τ_n with decreasing M_{PB}. Such a constant ratio of τ_n's of the two types of PI chains with and without dipole inversion was observed also for the bulk systems.[30] These results give an important clue in understanding the binary blend dynamics concerning the features of the competition of the constraint release and reptation mechanisms, as will be discussed in detail in Part 2 of this series.

It should be noted that the power-law dependence, $\tau_n \propto M_{PB}^3$, characteristic of the pure constraint release mechanism is not observed for the blends examined in Figure 6. This is because the matrix chains are not short enough and the constraint release process is not fast enough to

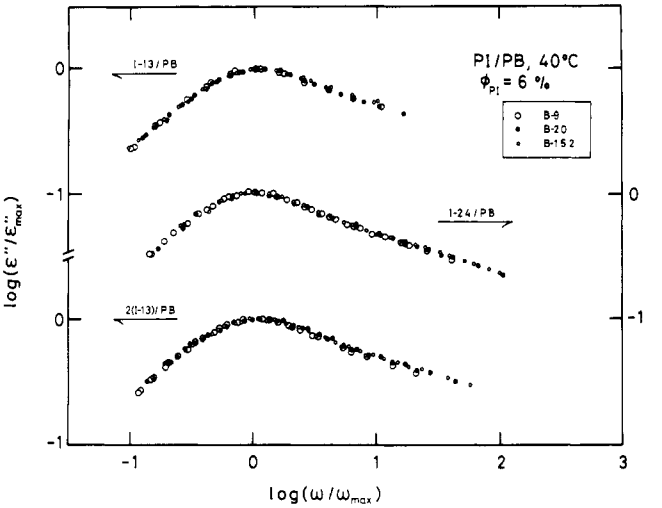

Figure 8. Comparison of the dielectric relaxation mode distribution (reduced ϵ'' curves) of I-13, I-24, and 2(I-13) (from top to bottom) in various PB matrices as indicated.

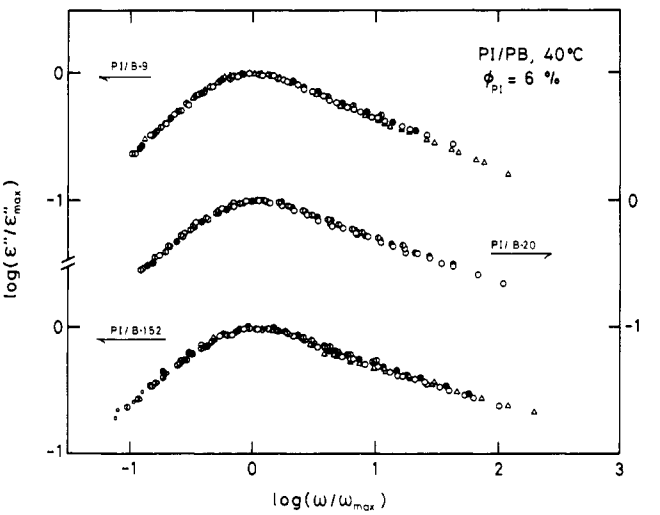

Figure 9. Comparison of the dielectric relaxation mode distribution for various PI chains in B-9, B-20, and B-152 matrices (from top to bottom). The symbols are the same as in Figure 4.

overwhelm reptation, as suggested from extensive rheological studies on similar blends.[10-14] From this point of view, the PI/PB blends examined are good model systems for examination of the competition of constraint release and reptation.

Relaxation Mode Distribution. Figure 8 compares the shape of $\epsilon''/\epsilon''_{max}$ versus ω/ω_{max} curves of I-13, I-24, and 2(I-13) chains (from top to bottom) diluted in various PB matrices as indicated. On the other hand, Figure 9 compares the reduced ϵ'' curves of different PIs blended with the same PBs. In these figures, we see that the mode distribution of the PI chains is insensitive to the matrix and probe molecular weights, M_{PB} and M_{PI}.[45] This insensitivity of the normal mode distribution to M_{PI} was found also for short PI chains blended in much longer PI matrices.[29] Such a universality of the dielectric normal mode distribution suggests that the competition of constraint release and reptation accerelates the dielectric relaxation of PI chains (as seen in Figure 6) *without affecting the mode distribution.*

Comparison of Behavior of PI/PB Blends and Bulk PI. Here we compare the dielectric normal mode relaxation behavior of narrow MWD probe PI chains in the present dilute PI/PB blends with that of narrow MWD PIs in the bulk state.[26,27,30] Before making such a

comparison, we make a few comments on the previous work on bulk PI systems.[21-30]

In earlier studies,[21-24] Adachi and Kotaka found significant broadening of ϵ'' curves of bulk PIs with increasing M_{PI} beyond M_c (M_c is the characteristic molecular weight for entanglements). They interpreted this broadening as a result of changes in the molecular motion due to entanglements and proposed a so-called three-τ model.[22] However, in a later careful reexamination of the problem using narrow MWD PIs (of $M_w/M_n < 1.1$),[26] they found that this broadening was due to a broad MWD of the samples used in the previous work[21-24] and discarded the three-τ model.

To examine the dielectric normal mode distribution of narrow MWD bulk PIs, Adachi, Kotaka, and co-workers estimated the Havriliak–Negami (HN) parameters for the *segmental modes* for respective PI systems. Using those parameters, they estimated the contribution of the segmental mode and subtracted it from the ϵ'' curve.[26] As seen in Figure 7a of ref 26, the subtraction little affected the ϵ'' curves of narrow MWD PIs with $10^{-3}M_{PI} = 13.5$, 31.6, and 52.9 at low $\omega < 100\omega_{max}$, with ω_{max} being the ϵ'' peak frequency. At those ω, the shape of the ϵ'' curves for those PI chains was found to be quite insensitive to M_{PI}. On the other hand, at high $\omega > 100\omega_{max}$, the subtraction changed the shape of the ϵ'' curves. After the subtraction, high-ω tails of the ϵ'' curve were found to become broader with increasing M_{PI} ($>M_c$).

The normal mode distribution of narrow MWD bulk PI, quite insensitive to M_{PI} at long time scales, *might* change with M_{PI} at short time scales, as Adachi, Kotaka, and co-workers concluded from the above results.[26] However, as judged from ambiguities in the estimated HN parameters (which were somewhat different from system to system[26]) and also from ambiguities in the above-mentioned subtraction, the difference in the ϵ'' curves *found after the subtraction* (<30% even at $\omega = 10^4\omega_{max}$; see Figure 7a of ref 26) may not be large enough to claim broadening of the normal mode distribution with M_{PI} at high ω. More importantly, the subtraction itself may be invalid because of the following difficulties. For PI chains, the dielectric normal and segmental modes, respectively, have been related to parallel and perpendicular components of the dipole of a PI segment.[20-26] Obviously, those two modes are induced by the same *local* motion. Thus, there would be a strong coupling for the time evolutions of the parallel and perpendicular dipoles at *short* time scales, possibly leading to difficulties for separation of the two modes (and the subtraction of ϵ'' due to the segmental mode) at high ω. Further investigation is necessary to understand the distribution of *fast* normal modes (due only to the parallel dipoles).

Here we compare the dielectric normal mode distribution in a frequency range, $\omega < 100\omega_{max}$, where we observe the dominant part of the slow relaxation. In this range, the contribution of the fast segmental modes to ϵ'' is negligible and its ambiguous subtraction[26] is not necessary. Figure 10 shows plots of log ($\epsilon''/\epsilon''_{max}$) against log ($\omega/\omega_{max}$) for narrow MWD PIs in bulk[26,27] (circles) and in the present dilute blends (solid curve). In Figure 10 we see that their normal mode distributions are close to each other and almost indistinguishable. We may conclude that the dominant part of the dielectric normal mode relaxation of narrow MWD PI chains exhibits a universal mode distribution, irrespective of their M_{PI} and entanglement environments such as whether they are in a monodisperse bulk state or in blends with various matrices.

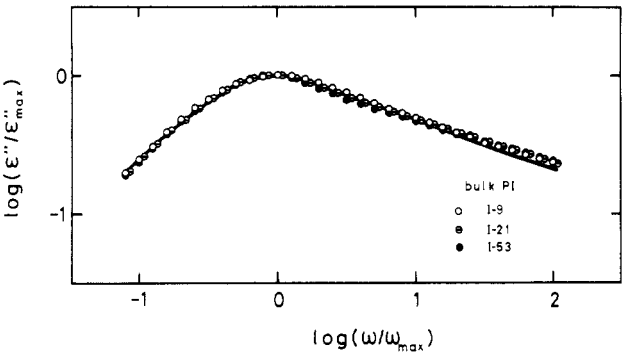

Figure 10. Comparison of the dielectric relaxation mode distribution of *narrow MWD* PI chains in bulk[26,27] (circles) and in dilute PI/PB blends examined in this study (solid curve). The molecular weights of the bulk PI samples are 9.49×10^3 (I-9; ref 27), 20.7×10^3 (I-21; ref 27), and 52.9×10^3 (I-53; ref 26).

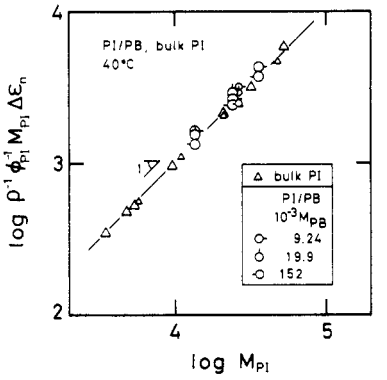

Figure 11. M_{PI} dependences of reduced relaxation intensities $\rho^{-1}\phi_{PI}^{-1}M_{PI}\Delta\epsilon_n$ at 40 °C for dielectric normal mode processes of PI chains in PI/PB blends (circles) and bulk PIs[26,27,30] (triangles). The large symbols indicate the data for regular PI chains (without dipole inversion), and the small ones, those for dipole-inverted PI chains.

For the dilute PI/PB blends examined here, we already found that the dielectric response is reflecting the motion of individual PI chains in the blends (cf. Figure 5). Thus, the universality of the mode distribution of the PI chains in bulk and in the blends found in Figure 10 supports the earlier suggestion of Adachi and Kotaka:[24] The dielectric response reflects the motion of individual PI chains, and the dot product $\langle \mu_i^p \cdot \mu_j^q \rangle$ with $p \neq q$ in eq 3 vanishes even in bulk PI systems.

For such a dielectric normal mode relaxation, the reduced relaxation intensity $\rho^{-1}\phi_{PI}^{-1}M_{PI}\Delta\epsilon_n$ is proportional to the mean-square end-to-end distance $\langle R^2 \rangle$ of the PI chain, as explained earlier (cf. eq 1'). Figure 11 compares the reduced intensities for the PI chains in the present blends (circles) with those for previously examined bulk PIs (triangles).[26,27,30,46] For the PI chains in the blends, $\Delta\epsilon_n$ were evaluated from Cole–Cole plots[18,26] of ϵ^* data and also by the following method. As seen from Figure 10, we can very well superpose the ϵ'' curves of the PIs in the blends on those of bulk PIs by shifting the former on double-logarithmic scales. The vertical shift factors necessary for this superposition represent the ratio of $\Delta\epsilon_n$ of the PIs in the blend and in bulk. Thus, $\Delta\epsilon_n$ of the PIs in the blends were evaluated from this factor and $\Delta\epsilon_n$ of bulk PIs (which were evaluated from the Cole–Cole plots and also from integration of ϵ'' with respect to log ω[26,27,30]). The $\Delta\epsilon_n$ for PI/PB evaluated by the above two methods coincided within experimental uncertainties.

As seen in Figure 11, the reduced relaxation intensities and thus $\langle R^2 \rangle$ of the PIs in the blends are close to those of bulk PIs and proportional to M_{PI}. This result strongly

suggests that the PI chains in the blends have a configuration close to the Gaussian configuration of the bulk PIs and are in a (nearly) unperturbed state.

Finally, a comparison of the absolute values of τ_n of PI chains in the dilute PI/PB blends and in bulk should also be interesting. However, at present, it is difficult to make this comparison on an unambiguous basis: First of all, it is difficult to adequately define an iso-segmental-friction state for PI chains in PI/PB blends and in bulk because of the ambiguity in determining the PI segment size in different environments. Although Figure 3 indicates that the friction of the probe PI segments in the PI/PB blends is determined by the motion of PB segments and is dependent only on temperature, the size and friction coefficient of a PI segment in a PB matrix, relative to those in bulk PI, are still unknown. In addition, the entanglement spacing necessary for making a meaningful comparison of τ_n is also unknown for the PIs in PB matrices. It is difficult to estimate this quantity without introducing any assumption. Because of those difficulties, we postpone a quantitative comparison of the absolute values of τ_n of PI chains in PB and in PI matrices to our future work.

V. Conclusion

For probe PI chains that are uniformly entangled with matrix PB chains and are in a (nearly) unperturbed state, we found τ_n decreases with decreasing matrix molecular weight M_{PB}. This result suggests that a competition is taking place between the constraint release and the reptation mechanisms. Thus, the situation for the PI chains in the PI/PB blends is similar to that in blends of chemically identical chains. The universality of the slow dielectric relaxation mode distribution (as judged from the insensitivity of the shape of the ϵ'' curves to M_{PI} and M_{PB} and/or to the environment seen in Figures 8–10) and the constant ratio of τ_n's of the two types of PI chains with and without dipole inversion may provide a clue in understanding how the two mechanisms compete and contribute to the dynamics of probe PI chains. Detailed discussion on this problem will be given in the following paper, Part 2, of this series.

References and Notes

(1) Graessley, W. W. *Adv. Polym. Sci.* **1974**, *16*, 1.
(2) Ferry, J. D. *Viscoelastic Properties of Polymers*, 3rd ed.; Wiley: New York, 1980; Chapter 13.
(3) See, for example, Chapter 10 of ref 2.
(4) Doi, M.; Edwards, S. F. *J. Chem. Soc., Faraday Trans. 2* **1978**, *74*, 1789, 1802, 1818; **1979**, *75*, 38.
(5) Doi, M.; Edwards, S. F. *The Theory of Polymer Dynamics*; Clarendon: Oxford, 1986.
(6) Graessley, W. W. *Adv. Polym. Sci.* **1982**, *47*, 67.
(7) Doi, M. *J. Polym. Sci., Polym. Phys. Ed.* **1983**, *21*, 667.
(8) Klein, J. *Macromolecules* **1978**, *11*, 852.
(9) Daoud, M.; de Gennes, P.-G. *J. Polym. Sci., Polym. Phys. Ed.* **1979**, *17*, 1971.
(10) Watanabe, H.; Kotaka, T. *Macromolecules* **1984**, *17*, 2316.
(11) Watanabe, H.; Sakamoto, T.; Kotaka, T. *Macromolecules* **1985**, *18*, 1436.
(12) Watanabe, H.; Kotaka, T. *Macromolecules* **1986**, *19*, 2520.
(13) Watanabe, H.; Kotaka, T. *Macromolecules* **1987**, *20*, 530.
(14) Watanabe, H.; Yoshida, H.; Kotaka, T. *Macromolecules* **1988**, *21*, 2175.
(15) Green, P. F.; Mills, P. J.; Palmstrøm, C. J.; Mayer, J. W.; Kramer, E. J. *Phys. Rev. Lett.* **1984**, *53*, 2145.
(16) Green, P. F.; Kramer, E. J. *Macromolecules* **1986**, *19*, 1108.
(17) Watanabe, H.; Tirrell, M. *Macromolecules* **1989**, *22*, 927.
(18) Stockmayer, W. H. *Pure Appl. Chem.* **1967**, *15*, 539.
(19) Baur, M. E.; Stockmayer, W. H. *J. Chem. Phys.* **1965**, *43*, 4319.
(20) Stockmayer, W. H.; Burke, J. J. *Macromolecules* **1969**, *2*, 647.
(21) Adachi, K.; Kotaka, T. *Macromolecules* **1984**, *17*, 120.
(22) Adachi, K.; Kotaka, T. *Macromolecules* **1985**, *18*, 466.
(23) Adachi, K.; Okazaki, H.; Kotaka, T. *Macromolecules* **1985**, *18*, 1486, 1687.
(24) Adachi, K.; Kotaka, T. *Macromolecules* **1988**, *21*, 157.
(25) Adachi, K.; Imanishi, Y.; Shinkado, T.; Kotaka, T. *Macromolecules* **1989**, *22*, 2391.
(26) Imanishi, Y.; Adachi, K.; Kotaka, T. *J. Chem. Phys.* **1988**, *89*, 7585.
(27) Yoshida, H.; Adachi, K.; Watanabe, H.; Kotaka, T. *Polym. J.* **1989**, *21*, 863.
(28) Adachi, K.; Yoshida, H.; Fukui, F.; Kotaka, T. *Macromolecules* **1990**, *23*, 3138.
(29) Adachi, K.; Itoh, S.; Nishi, I.; Kotaka, T. *Macromolecules* **1990**, *23*, 2554.
(30) Yoshida, H.; Watanabe, H.; Adachi, K.; Kotaka, T. *Macromolecules* **1991**, *24*, 2981.
(31) Boese, D.; Kremer, F. *Macromolecules* **1990**, *23*, 829.
(32) Boese, D.; Kremer, F.; Fetters, L. J. *Makromol. Chem., Rapid Commun.* **1988**, *9*, 367; *Macromolecules* **1990**, *23*, 1826.
(33) Hasegawa, H.; Sakurai, S.; Takenaka, M.; Hashimoto, T.; Han, C. C. *Macromolecules* **1991**, *24*, 1813.
(34) Cole, R. H. *J. Chem. Phys.* **1965**, *42*, 637.
(35) Olabisi, O.; Robeson, L. M.; Shaw, M. T. *Polymer–Polymer Miscibility*; Academic Press: New York, 1979; Chapter 2.
(36) de Gennes, P.-G. *Scaling Concepts in Polymer Physics*; Cornell University Press: Ithaca, NY, 1979; Chapter IV.
(37) Hasegawa and co-workers[33] reported that blends of deuterated PB and protonated PI exhibit a lower critical solution temperature (LCST). A similar behavior is expected for our PI/PB blends (containing only protonated species), although not confirmed in a limited range of temperatures examined in Figure 2. (Because of the isotope effect, the LCST itself may be different for blends containing protonated and deuterated PB.[33])
(38) Jelenic, J.; Kirste, R. G.; Oberthur, R. C.; Schmitt-Strecker, S.; Schmitt, B. J. *Makromol. Chem.* **1984**, *185*, 129.
(39) Hadziioannou, G.; Stein, R. S. *Macromolecules* **1984**, *17*, 567.
(40) Shibayama, M.; Yang, H.; Stein, R. S.; Han, C. C. *Macromolecules* **1985**, *18*, 2179.
(41) Bates, F. S.; Fetters, L. J.; Wignall, G. D. *Macromolecules* **1988**, *21*, 1086.
(42) Maconnachie, A.; Fried, J. R.; Tomlins, P. E. *Macromolecules* **1989**, *22*, 4606.
(43) Colby, R. H.; Fetters, L. J.; Graessley, W. W. *Macromolecules* **1987**, *20*, 2226.
(44) A referee for this paper interpreted the increase of relaxation times τ_n of PIs with increasing M_{PI} as due to a critical slowing down that becomes significant as M_{PI} increases and the spinodal is approached. However, at the experimental conditions, all blends are far from the spinodal and the PI chains are in a (nearly) unperturbed state, as shown in Figures 2 and 11. In addition, *if* a critical slowing down were the cause of the increase of τ_n, the dependence of τ_n on matrix molecular weight M_{PB} should become stronger as M_{PB} increases and the blend approaches the spinodal. This is opposite to the experimental results shown in Figure 6. Thus, the M_{PI} and M_{PB} dependence of τ_n of the PIs in the present blends cannot be attributed to a critical slowing down. Instead, it is related to competition of some relaxation mechanisms, as in the case of blends of chemically identical chains. Within the framework of the generalized tube model, competition of the constraint release and reptation mechanisms should be considered.
(45) The dielectric normal mode distribution of PI chains is affected by MWD and also by the distribution of the location of the dipole inversion point. We made a detailed comparison of ϵ'' curves considering those distributions for PI chains with and without dipole inversion.[30] However, for the narrow MWD PI chains examined in this study, changes of ϵ'' curves due to those distributions, if any, are small. In fact, we see little difference of the mode distribution in Figures 8 and 9.
(46) For narrow MWD PIs having sharp ϵ'' curves, the fast normal modes observed at $\omega > 100\omega_{max}$ make only a minor contribution (<10%) to $\Delta\epsilon_n$ (cf. Figure 9 of ref 26). Thus, an ambiguity for the fast modes resulting from the problem of the subtraction of the segmental mode contribution from ϵ'' at high ω hardly affects the discussion for $\Delta\epsilon_n$.

Registry No. PI, 9003-31-0; PB, 9003-17-2.